3D SELECTION OF ENVISAT DATA FOR IMPROVED WATER STAGE TIMES SERIES ON THE RIO NEGRO AND ADJACENT WETLANDS (AMAZON BASIN)

Joecila Santos da Silva[1,2], Emmanuel Roux[3], Otto Corrêa Rotunno Filho[1], Marie-Paule Bonnet[3], Frédérique Seyler[3] and Stéphane Calmant[2]

1 : Programa de Engenharia Civil – COPPE
Universidade Federal do Rio de Janeiro – UFRJ
Caixa Postal 68506
21945-970, Rio de Janeiro, Rio de Janeiro, Brasil.

2 : Laboratoire d'Etudes en Géophysique et Océanographie Spaciales – LEGOS (CNES/CNRS/IRD/UPS/OMP)
14 avenue Edouard Belin
31400, Toulouse, France.

3 : Laboratoire des Mécanismes et Transferts en Géologie – LMTG, (CNRS/IRD/OMP/UPS)
14 avenue Edouard Belin
31400, Toulouse, France.

Corresponding author. E-mail addresse: joecila.silva@ird.fr (J. S. Silva)

ABSTRACT

Time series of water stages derived from satellite radar altimetry are of very variable quality, depending on the mission, the tracking scheme and the geomorphological context of the crossing between the satellite track and the river. Also, it has long been observed that this quality is dependent on the hydrological cycle itself: stage values are often much worse at low water compared to those determined at high waters. This problem is mostly due to the data selection. Indeed, common window for data selection is mostly geographical. At low waters, measurements contaminated/distorted by non-water reflectors are more likely present within the selection window because of emerged river banks and/or islets. We have developped a processing scheme based on the GRASS freeware GIS to improve the selection of the satellite measurements and reduce the incorporation of non-water measurement within the dataset retained for estimating the water stage. This scheme has been successfully applied to the ENVISAT mission over the Rio Negro where reliable water stages could be obtained far upstream at both high and low waters, and also over adjacent wetlands.

Key-words: Spatial altimetry, Rio Negro basin, water level.

Introduction

In the last decades, the demand for answering more challenging questions related to the study of climate modifications posed a series of issues about the understanding of hydrological systems. This type of scientific problem requires knowledge of how physical processes take place and occur under a framework that includes different spatial and temporal scales jointly with physical constraints. Understand and forecast the effect of climate changing requires that we understand the hydrological basin as a component of a broad system, which is dynamic and highly complex, including in particular in temporarily inundated zones that play an important role in the local hydrological cycle (Birkett, 1995). Among these hydrological systems, the Amazon is one of the most important. The Amazon basin is characterized by its large drained area (37% of South America), together with the low altitude of the alluvial plain that presents a very mild average slope (1cm/km) (Guyot *et al*. 1993 and 1994). Consequently, it is made up of a complex net of lakes more or less connected to the main river channels and covering areas estimated between 60 000 km2 (Sippel *et al*. 1998) and 300 000 km2 (Junk, 1983). During flooding season, waters of main stems drain into these lakes and remain there for several months. As a consequence, this outpouring modifies the flood peak of the rivers. In the dry season, the water stored in the flooded plains is released, leading to an increase of the drought. These great lakes work as natural reservoirs affecting the hydrological cycle of the main Amazon River channel and main tributaries and therefore, that of the global hydrological cycle. As many other large tropical basins, the Amazon basin is poorly monitored and lacks stage information for all the aforementioned components of the hydrographic network. Then, getting time series of water stage by means other than readings at local gauges is mandatory. Therefore, this study

focuses on building time series of water stage using satellite altimetry for the large rivers channels, reduced-size tributaries and wetlands within a sub-basin of the Amazon basin, the Rio Negro basin. The ~2000 km long Negro River is the second river in the world in terms of water volume (IBAMA, 2007). Its basin drains approximately 700.000Km², ~ 10% of the entire Amazon Basin. It starts so-called Chamusiqueni river in the plateau of Guainia Comissary, Republic of Colombia, at ~180m of altitude. Its name next turns to Guainia River in the Colombia and Venezuela central lands and last changes to Negro river in the Brazilian Amazon, after its confluence with the Casiquiare River at the Brazil-Venezuela boundary. The riverbed roughly trends southeastwards until its junction with the Solimões River at Manaus. Its main climatic characteristics are listed in Table 1.

Satellite altimetry and the ENVISAT mission

Altimetry radars installed on board of various satellite missions emit a pulse towards the nadir and receives the echo reflected by the water surface level. Echo analysis permits to extract the distance between the satellite and the reflector, so called range R. Owing to the fact that the satellite altitude H with respect to a reference ellipsoid is known accurately by orbitography modeling, the height of the reflector with respect to that geodetic reference is given at each pass of the satellite by: (Eq. 1).

$$h = H - R + \sum_{j} \Delta R_j \qquad (1)$$

Where □Rj are environmental – propagation through the troposphere and ionosphere – and geophysical corrections – tides – (Fu and Cazenave, 2001).

In the frame of the Earth Observation Program, the European Spatial Agency (ESA) launched the satellite ENVironmental SATellite (ENVISAT) in March, 2002. It is the biggest satellite for Earth observation built until now. Data collected by ENVISAT are dedicated for Earth environmental and climate change analyses. ENVISAT embarks 10 instruments that allow a strict analysis of atmosphere, continents, oceans and ice of the planet (Wehr and Attema, 2001) including a nadir radar altimeter (RA-2 or Advanced Radar Altimeter). ENVISAT orbits a helio-synchronous circular orbit with an inclination of 98.5° and a 35 day repeat period. It fulfills a global cover of Earth within latitudes of ± 82.4° and an intertrack distance of approximately 80 Km at the Equator.

ENVISAT embarks RA-2, a high precision radar pointing towards the nadir and operating in two frequencies (Zelli, 1999), *e.g.* at 13.575 GHz (2.3 cm wavelength, Ku band) and at 3.2 GHz (3.4 cm wavelength, S band). This dual-frequency system enables estimating the ionospheric delay. The width of the ground footprint is approximately 3.4 km.

Virtual Stations and altimetry data processing

A virtual station consists in the intersection of a satellite track with a water body, making possible to derive time series of the water stage variations from the radar measurements at each pass. However, all the radar measurements a priori returned by a water surface are not necessarily valid measurements. Indeed, several factors may affect the measurement among which the most frequent are:

+ non-water reflectors such as banks, islets, vegetation, etc… may have bounced significant energy together with the water surface and affect the computation of the range;

+ the water surface at the rim of the footprint may dominate the energy received by the satellite although the latter is not right over the water body (so-called “hooking” artifact) and translate to an apparently valid – but slant- range.

In order to overcome these problems in the selection of the data to be included in the estimate of a water height, we have developed a methodology to altogether geographically and visually select the altimetry data at the virtual stations. The VALS software (VALS standing for Virtual ALtimetry Station) consists in routines developed in the frame of the GRAS GIS 6.1 freeware SIG. The data processing is performed in three main steps:

+ Rough selection guided by imagery (Figures 2a, 3a and 4a). The along track measurements are displayed over a geo-referenced image chosen such as to highlight the wet and dry areas in the vicinity of the studied virtual station. The measurements in the close vicinity of the water surface – as shown by the image – are selected and passed to the second step. In the present study the images we used were mosaics of JERS-1 radar interferrometry produced in the frame of the tropical forest global mapping – Global Rain Forest Mapping-GRFM projects (GRFM 1995/1996). Both low waters and at flood periods are available. We used the flood period images.

+ Refined selection in cross section (Figures 2b, 3b and 4b). The data selected in the first step are now displayed in a height/cross-section abscissa diagram. Again, the operator can draw a polygon inside which the data are retained. Noteworthy, several disconnected polygons can be defined.

+ Computation of master points. The median and mean values are computed for each pass using the data subset selected in the second step. In the present study, we retained the median and associated mean absolute deviation to construct the time series. Indeed, we have experienced that given the large

number of possible outliers with respect to the little number of points selected for each pass, the median offers a more robust predictor than the mean would do. Frappart et al. (2006) already arrived at a similar conclusion.

Using the VALS toolbox for the ENVISAT tracks crossing the Negro river bassin, we computed time series of water stage between 2002 and 2006 at about 150 virtual stations. As far as the ENVISAT data are concerned, we used the ranges issued by the Ice-1 algorithm and geophysical corrections provided in the standard GDRs, but the tropospheric corrections that are post processed using meteorological models. Among the 4 ranges distributed in the ENVISAT GDRs, The Ice-1 ranges option has been retained following Frappart *et al.* (2006) who showed that Ice-1 was the algorithm performing best for continental waters. The 150 virtual stations include 34 stations on the river main stem, 66 over tributaries and 50 over wetlands. Their locations are shown in Figure 1. We present examples of series obtained for these three types of water body: a large river, a small tributary and a wetland. The data selection and time series of a virtual station in the Anavilhanas Islands, where track 637 crosscuts the Rio Negro in its widest portion, is shown in Figure 2. As shown on the cross-section, the width of the river changes significantly between the low and high water. This case highlights the great advantage provided by a supervised data selection that enables on the one hand selecting smaller portions of tracks at low water to eliminate the data on the river bank but on the other hand select all the data at high waters and take advantage of the large number of samples at these measurement times. The case of a small tributary is shown in Figure 3. The virtual station is on the Pardo River, a river 300 to 400 m wide, that is narrower than the beam footprint, crosscut by track 149. It is worth noting that larger deviations are associated to the height values than for the Rio Negro. Noteworthy,

this river is not monitored and then could not be taken into account in any hydrological modeling until these ENVISAT series were computed. Last, we present a series extracted where track # 235 passes over a wetland, the Caapiranga Lake (297.48 °E and 0.63 S) (Figure 4). Wetlands are poorly monitored worldwide. Indeed, it appears almost infeasible to monitor locally the stage variations of such remote areas and the surface-integrating capability of the radar beam is an advantage in this case and permits the computation of stage variations.

Given the very small number of gauges along the main stem of Rio Negro, only one virtual station is located in the very close vicinity of a gauge (*e.g.* the São Felipe station, 700m away only from the ENVISAT track). A single series is not satisfactory to address the problem of the quality of the ENVISAT series by comparison with a gauge series. Therefore, in order to perform such a comparison on the basis of several pairs of series, we also computed the time series of water stages at 5 other ENVISAT virtual stations that are located less than 20 km from a gauge within the Amazon basin (Table 2), including two other stations along the Negro basin. Comparison between ENVISAT time series and gauge time series is presented in Figure 6. First, we computed the weighted linear regression between both series at each gauge-SV pair. Regression coefficients range between 1.002 and 0.59 (Table 3). Yet, when this coefficient is close to one, it is suggested that both series agree very well. However, a value significantly different from one does not indicate that the ENVISAT series is necessarily bad. It can also evidence that hydrological conditions are different between both locations. Therefore, we also computed the ratio χ between on the one hand the discrepancy between the ENVISAT master points and the linear regression and on the other hand uncertainties associated to the ENVISAT master points (see formula in the caption of Table 3). When χ equals one, the uncertainties are not under-estimated.

When χ is greater than one, the uncertainties must be scaled by χ to globally range as much as the discrepancies do. The χ value for the comparison at every ENVISAT/gauge pair is reported in Table 3. Values range between 1 (Barcelos) and 7 (São Paulo de Olivença). This means that the uncertainties of the ENVISAT virtual station at Barcelos are realistic when those for the virtual station at S-P de Olivença are 7 times under-estimated. At Jatoba, that $\chi = 3.6$ suggests that the ENVISAT series compares as well the corresponding in-situ series as the other series do, and also suggest that the low regression coefficient (0.590) is due to a significant change in river cross section between the location of the SV and that of the gauge. When computed globally for all the stations, $\chi = 3.6$. This suggests that realistic uncertainties are obtained for ENVISAT series when those issued by our selection procedure are multiplied by 3.6.

At Obidos, two gauges are available. We also compared these two gauges together. The regression coefficient between both gauges is 0.966 and $\chi = 30$, using a 1 cm uncertainty to characterize the gauge readings (Table 3). Such values, that suggest that the actual uncertainty of the reading is 30 cm are surprisingly bad. Yet, inspection of the data series suggests that a measurement in the auxiliary series is likely wrong (either because of a reading error or because of an erroneous transcription). This outlier is circled in Figure 6. Thus, if this data is removed from the series, the correlation rises up to 0.995 and $\chi = 3$ (Table 3), suggesting that the actual uncertainty of the readings is ~3 cm.

The gauges that we used were not leveled. Such linear regressions between gauges series and ENVISAT series that are referenced with respect to the WGS84 ellipsoid enable to level the gauge zeros. However, such levelling using satellite radar altimetry must accounts for the fact that the ranges drived by the Ice-1 trackers are potentially biased. Since no value has yet been published for the Ice-1

tracker bias over the rivers, we used the value determined by Cretaux *et al.* (submitted) over Lake Issyk-kul, namely 72.6 cm ± 5 cm. The levels of the zeros of the gauges included in this study are reported in Table 3. These values might need to be updated when a river-dedicated estimate of the bias is available.

Conclusion and perspectives

Large –metric– errors often observed in time series constructed using satellite radar altimetry are proceeding of the difficulties found to adapt measurement and processing procedures tuned for the oceanic domain. Most of the errors come from the inclusion of non-water data in the set of measurements retained for the computation of water stages, in particular at low water stages (Birkett, 1998; De Oliveira Campos 2001). Most of this scatter can be dramatically reduced if a supervised selection of the data is performed prior the computation of the master points making the final time series. The method that we propose to perform such a selection consists in adding to the common geographical selection a second step of data selection, in a cross-section view. After some satellite passes are available, such cross section displays permit a satisfactory identification of non-water measurements, hooking disturbances and change with hydrological cycle in the width of the geographical selection window.

Unfortunately, no comparison could be performed over small tributaries or wetlands; the most demanding places and this test remains to be performed. Yet, a comparison performed at six gauges over different rivers within the Amazon basin result in regression coefficient greater than 0.95 between the ENVISAT and gauges series. Uncertainties appear under-estimated and a 3.6 scaling factor is proposed. Although such a study requires to be conducted over a much larger

dataset for definite conclusions are drawn, it is shown that ENVISAT altimetry provides valuable measurements of the water level, of particular interest in poorly monitored areas such as the Amazon basin.

Acknowledgements

This study was partly funded by TOSCA/CNES (France), CNPq (Conselho Nacional de Desenvolvimento Científico e Tecnológico, Brazil) and CAPES (Coordenação de Aperfeiçoamento de Pessoal de Nível, Brazil, contract CAPES/COFECUB Nº 516/05). ANA (Agência Nacional de Águas, Brazil) provided the gauge data and *CTOH* (*Centre de Topographie des Océans et de l'Hydrosphère, LEGOS, France*) provided the ENVISAT *GDRs* and additional troposheric corrections.

References

BIRKETT, C. M. (1995). The global remote sensing of lakes, wetlands and rivers for hydrological and climate research. *IEEE Trans.* 1979–1981.

BIRKETT, C. M. (1998). Contribution of the TOPEX NASA radar altimeter to the global monitoring of large rivers and wetlands, *Water Resour. Res.,* 34 (5), 1223-1239.

BRASIL. Departamento Nacional de Produção Mineral. Projeto RADAMBRASIL. (1978). *Manaus: Geologia, Geomorfologia, Pedologia, Vegetação e Uso Potencial da Terra.* Rio de Janeiro: DNPM, 18, AS. 20, 628p.

CRETAUX, J. F.; S. CALMANT; V. ROMANOVSKI; A. SHABUNIN ; F. LYARD ; M. BERGE-NGUYEN; A. CAZENAVE and F. HERNADEZ. (2007). A new absolute calibration site for radar altimeter in the continental domain: lake Issykkul in Central Asia. Submitted to Journal of Geodesy.

DUBROEUCQ, D. and B. VOLKOFF. (1998). From oxisols to spodosols and histosols: evolution of the soil mantles in the Negro River basin (Amazonia). *Catena.* 32, 245–280.

FRAPPART, F.; S. CALMANT; M. CAUHOPÉ; F. SEYLER and A. CAZENAVE. (2006) Preliminary results of ENVISAT RA-2-derived water levels validation over the Amazon basin. *Remote Sensing of Environment*. 100, 252–264.

FU, L. L. and A. CAZENAVE. (2001). *Satellite Altimetry and Earth Science, A Handbook of Techniques and Applications*. London (UK), Academic Press., 464p.

GUYOT, J. L. (1993). Hydrogéochimie des fleuves de l'Amazonie Bolivienne. In: *Géologie, Géochimie*, Bordeaux, Université Bordeaux I, 261p.

GUYOT, J.L.; M. MOLINIER; E. DE OLIVEIRA; V. GUIMARAES and A. CHAVES (1993). Hydrologie du Bassin de l'Amazone. In : OLIVRY, J. C. et BOULEGUE, J. (eds) : *Grands bassins fluviaux péri-atlantiques : Congo, Niger, Amazone*. Actes du Colloque PEGI/INSU/CNRS. ORSTOM, Paris, France, 22-24 novembre 1993, 335-344.

GUYOT, J. L.; M. MOLINIER; V. GUIMARAES; K. CUDO and E. DE OLIVEIRA. (1994). Nouveautés sur les débits monstrueux de l'Amazone. *Dossier de la Revue de Géographie Alpine*, 12, 77-83.

GRFM (1995/1996). *Global Rain Forest Mapping Project, South America (Amazon Basin)***,** v. AM-1, National Space Development Agency of Japan /Earth Observation Research Center (NASDA/EORC), Japão.

IBAMA. Instituto Nacional do Meio Ambiente e dos Recursos Naurais Renováveis. (2007). *Região hidrográfica amazônica.* In: www.ibama.gov.br/pndpa/index.php?id_menu=71

JUNK, W. J. (1983). As águas da Região Amazônica. In: SALATI, E. *et al. Amazônia: desenvolvimento, integração e ecologia*. São Paulo: Brasiliense; (Brasília): Conselho de Desenvolvimento Científico e Tecnológico, 45-100.

DE OLIVEIRA CAMPOS, I .; F. MERCIER; C. MAHEU; G. COCHONNEAU; P. KOSUTH; D. BLITZKOW and A. CAZENAVE A. (2001). Temporal variations of river basin waters from Topex/Poseidon satellite altimetry ; application to the Amazon basin, *C.R. Acad. Sci. Paris, Sciences de la Terre et des planètes.* 333, 1-11.

SIPPEL, S. J.; S. K. HAMILTON; J. M. MELACK and E. M. L. M. NOVO (1998). Passive microwave observations of inundation area and the area/stage relation in the Amazon River floodplain. *International Journal of Remote Sensing.* 19, 3055–3074.

SOIL SURVEY STAFF (1975). Soil Taxonomy. *Basic System of Soil Classification for Making and Interpreting Soil Surveys.* USDA, Washington, Agricultural Handbook. 436, 754 pp.

SOIL SURVEY STAFF (1990). Keys to Soil Taxonomy. Agency for International Development. USDA Soil Management Support Services.

Technical Monograph 19, fourth ed., Virginia Polytechnic Institute and State University.

WEHR, T. and E. ATTEMA. (2001). Geophysical validation of ENVISAT data products, *Adv. Space Res.* 28 (1), 83-91.

ZELLI, C. (1999). ENVISAT RA-2 advanced radar altimeter: Instrument design and pre-launch performance assessment review, *Acta Astronautica.* 44, 323-333.

Table 1 : Main characteristics of the Rio Negro basin

Bacia do rio Negro	
Area	715 000 Km²
Climate	Am*, Af** and Aw***
Mean annual temperature	26 °C
Mean annual precipitation	3 000 – 4 000 mm
Period of main precipitation	April to June
Mean discharge at mouth	~50 000 m³/s

From BRASIL (1999), Dubroeucq e Valkoff (1998), Guyot (1993) and Soil Survey Saff (1975, 1990).

* : Am : Hot and humid with dry winter.

** : Af : Hot and humid with no dry season.

*** : Aw : Hot and humid with short dry season.

Table 2 : Characteristics of the gauge stations used for comparison with Virtual stations

Gauge		River	Longitude (°)		Latitude (°)		D (Km)*
Name	**ID**		**Virtual**	**Gauge**	**Virtual**	**Gauge**	
São Felipe	14250000	Negro	292.667	292.687	0.277	0.372	- 0.7
Barcelos	14480002	Negro	297.087	297.069	-0.864	-0.966	+11
Manaus	14990004	Negro	299.836	299.973	-3.069	-3.137	+17
São Paulo de Olivença	11400000	Solimões	291.129	291.250	-3.445	-3.450	+ 4
Óbidos (Linígrafo)	17050001	Amazon	304.513	304.487	-1.955	-1.919	- 5.6
Óbidos (Auxiliary)	17050002	Amazon	304.513	304.489	-1.955	-1.947	-3.4
Jatobá	17650000	Tapajós	303.073	303.146	-5.199	-5.152	-9

* : Sign + stands for the virtual station being upstream the gauge, sign – stands for the virtual station being downstream the gauge

Table 3: Statistics of the comparison between the virtual stations and neighboring gauges

Station name	**$A \pm \sigma_A$**	**$H_0 \pm \sigma_H$ (m)**	**χ (1)**	**E_z (m) (2)**
São Félipe	0.970 ±0.005	63.404 ± 0.048	2.9	62.678 ± 0.16
Barcelos	0.976 ±0.010	10.742 ± 0.073	1.0	10.016 ± 0.09
Jatoba	0.590 ± 0.002	30.385 ± 0.016	3.6	29.659 ± 0.08
Manaus	1.002 ± 0.005	-18.000 ± 0.123	2.3	-18.726 ± 0.29
SP Olivença	0.966 ± 0.003	60.286 ± 0.029	7.1	59.560 ± 0.22
Óbidos (Limni)	0.904 ± 0.01	-17.173 ± 0.031	1.6	-17.899 ± 0.07
Óbidos (Auxiliary)	0.867 ± 0.01	-17.082 ± 0.031	4.7	-17.808 ± 0.07
Óbidos/Óbidos A: all values B: outlier removed	0.965 ± 0.001 0.995 ± 0.001		(3) 30 3	

(1): $\chi = \sqrt{\dfrac{\sum_N \dfrac{\left[H_{env} - \hat{H}\right]^2}{\sigma^2}}{N-2}}$ where $\hat{H}$ is the height computed from the best fitting linear regression.

(2) : Ez stands for the Ellipsoidal height of the gauge zero (in m with respect to WGS 84). Associated uncertainties account for both σ_H and the bias uncertainty published by Cretaux et al. (submitted).

(3) : An a priori 1 cm uncertainty was assumed for all the in-situ measurement for the weighted regression in this particular case.

Figure Captions

Figure 1: map of the Rio Negro basin together with the virtual stations defined by the intersection of the river channels with the ground tracks of satellite ENVISAT. In situ stations used in this study are also shown. Background image is a JERS-1 mosaic made of images 304-305-306-311-312-313, e.g. Amazon high water images.

Figure 2: Virtual station on the Rio Negro at 297.41; -1.05, ENVISAT track # 736.
A: Display of the geographical distribution of the data selected
B: time series

Figure 3: Virtual station on the Rio Pardo (299.44; -1.74), ENVISAT track # 149.
A: Display of the geographical distribution of the data selected
B: time series

Figure 4: Virtual station on the Lago Caapiranga (297.48; - 0.63), ENVISAT track # 235.
A: Display of the geographical distribution of the data selected
B: time series

Figure 5: Comparison of water levels from both processing the altimetry data of ENVISAT track # 536 at latitude 0.37 and readings at São Felipe gauge station ANA 14250000.

Figure 6: Comparison between the ENVISAT and the gauges values. Red lines stand for the best fitting regression lines. The coeficients of the linear regressions are reported in Table 3.

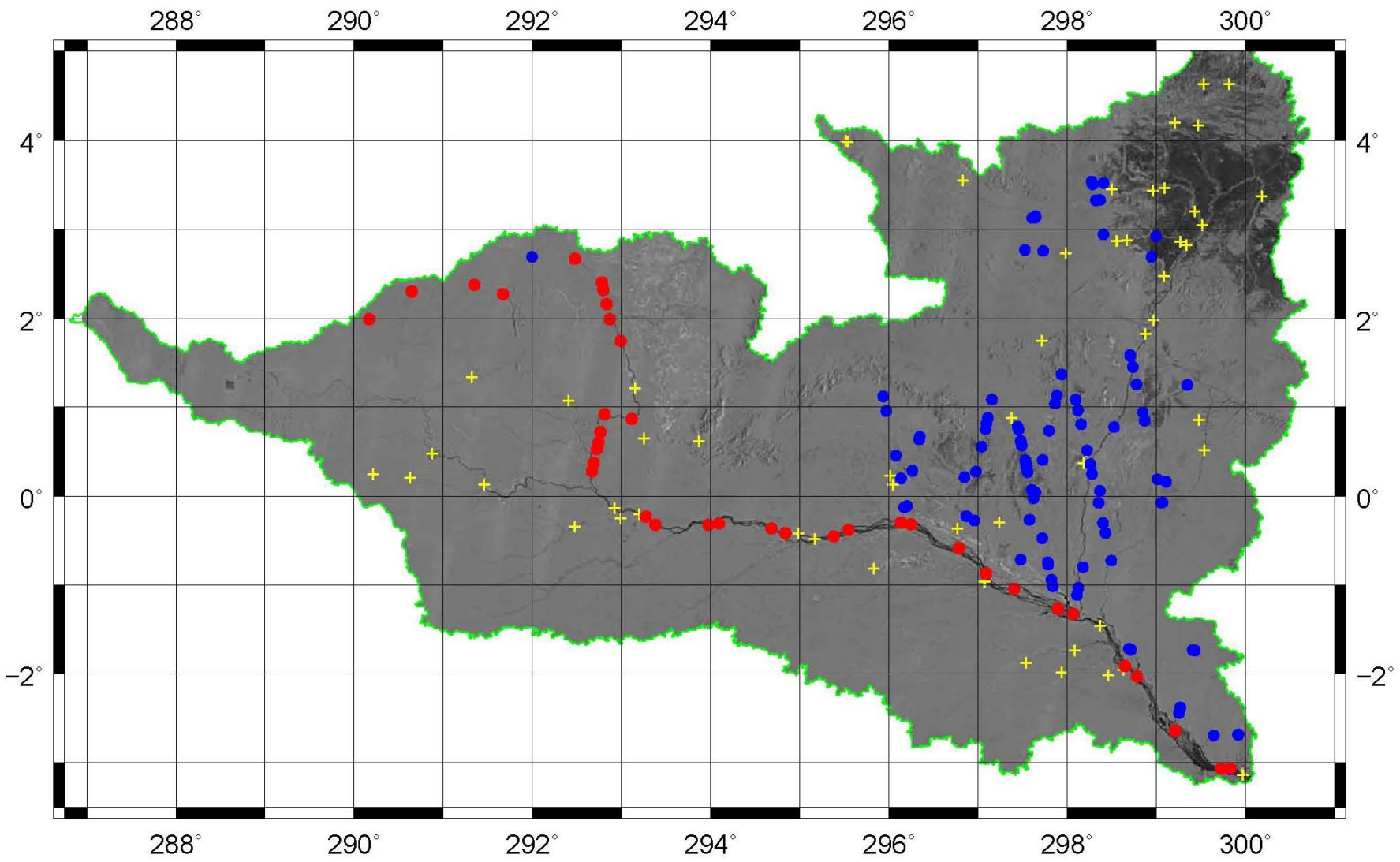

Figure 1

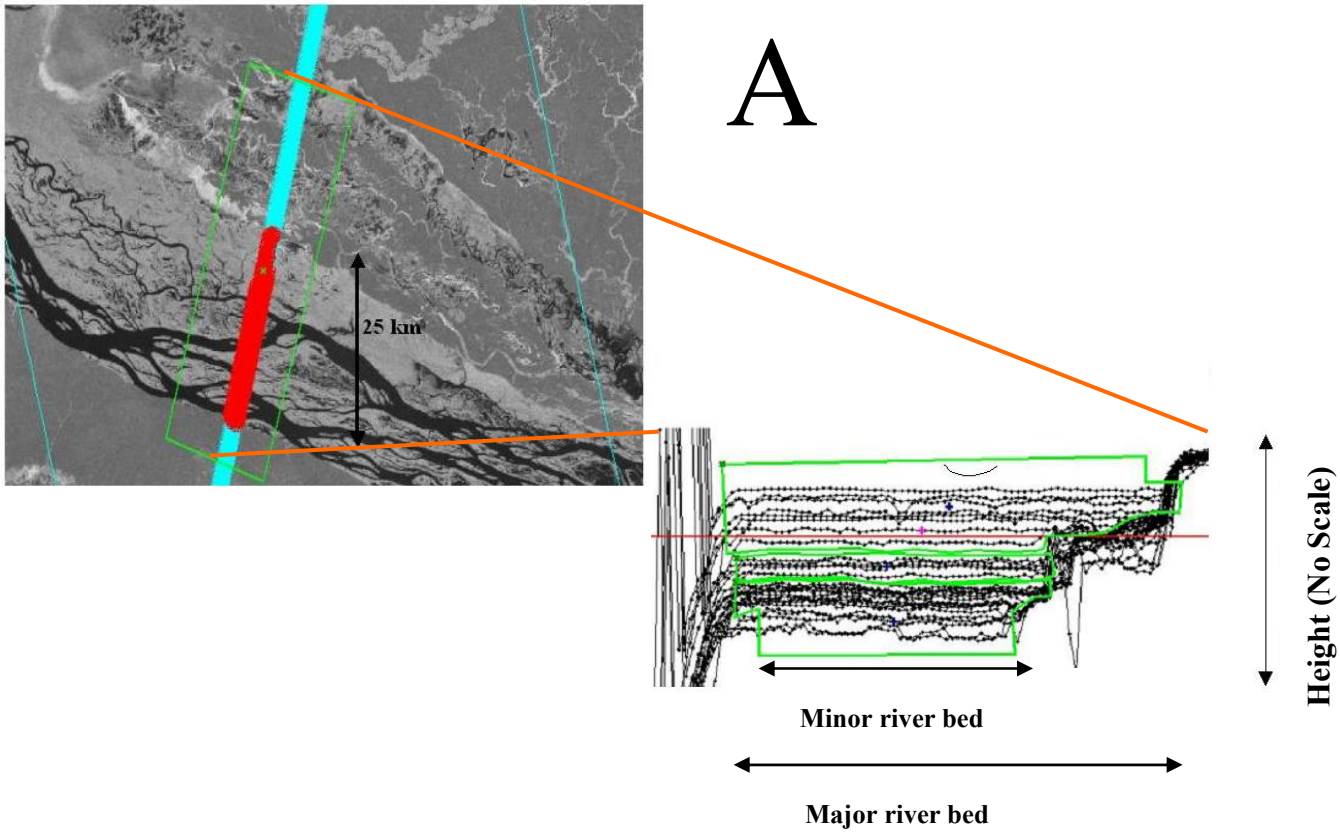
A
25 km
Height (No Scale)
Minor river bed
Major river bed

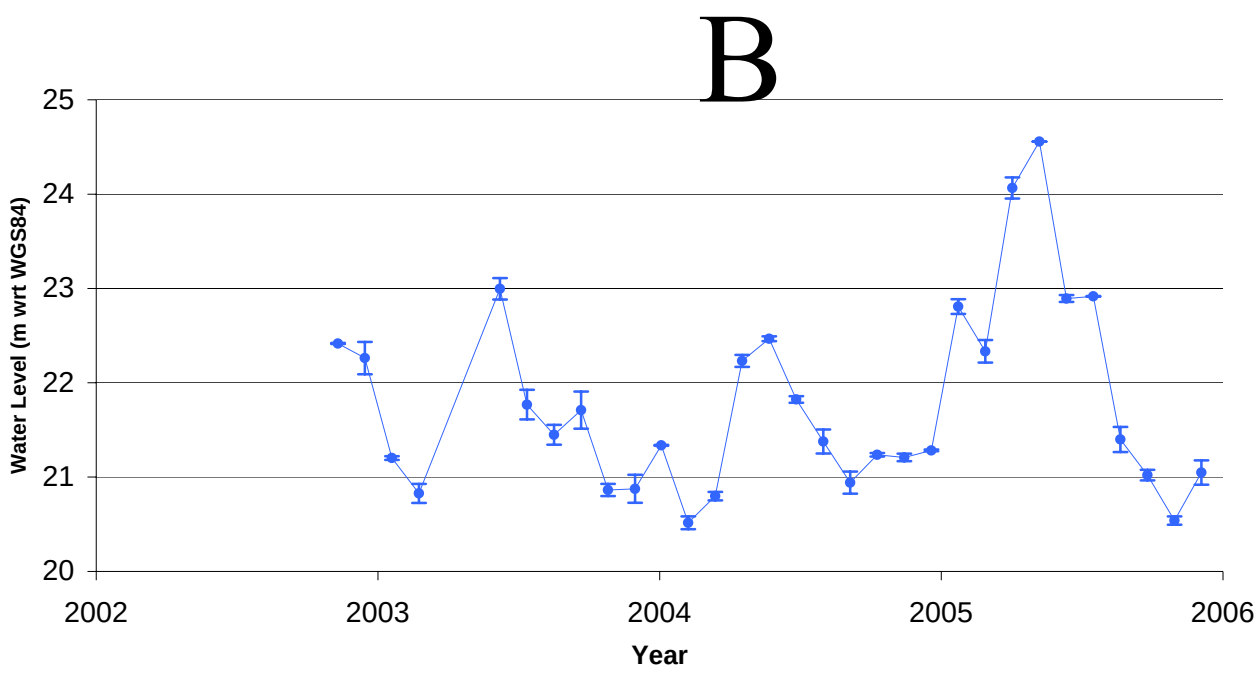
B
Water Level (m wrt WGS84)
25
24
23
22
21
20
2002
2003
2004
2005
2006
Year

Figure 2

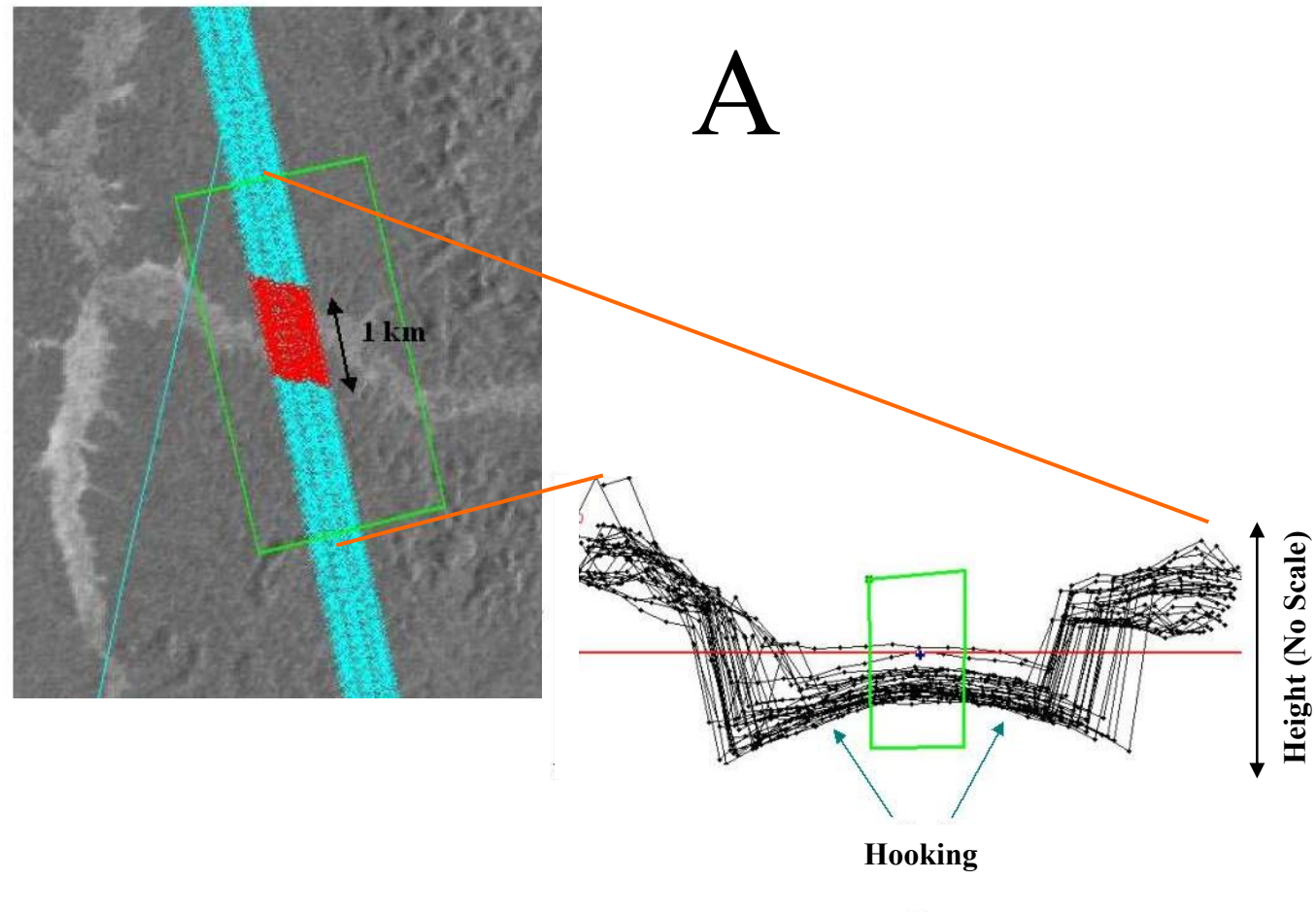
A
1 km
Height (No Scale)
Hooking

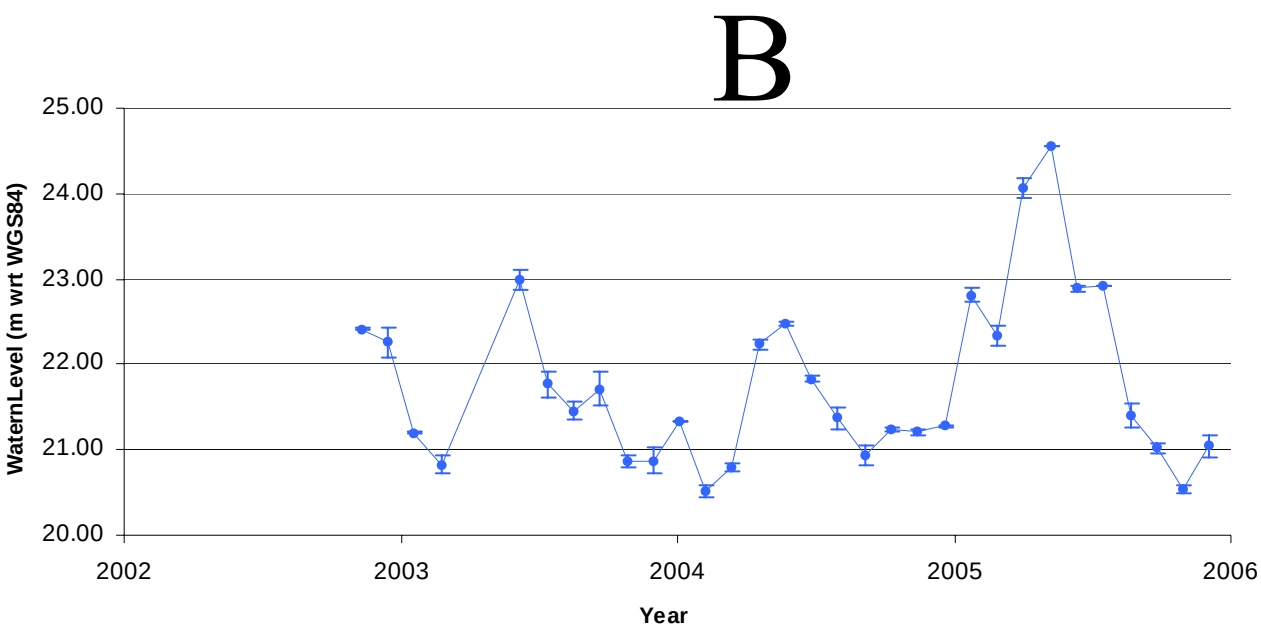
B
WaternLevel (m wrt WGS84)
25.00
24.00
23.00
22.00
21.00
20.00
2002
2003
2004
2005
2006
Year

Figure 3

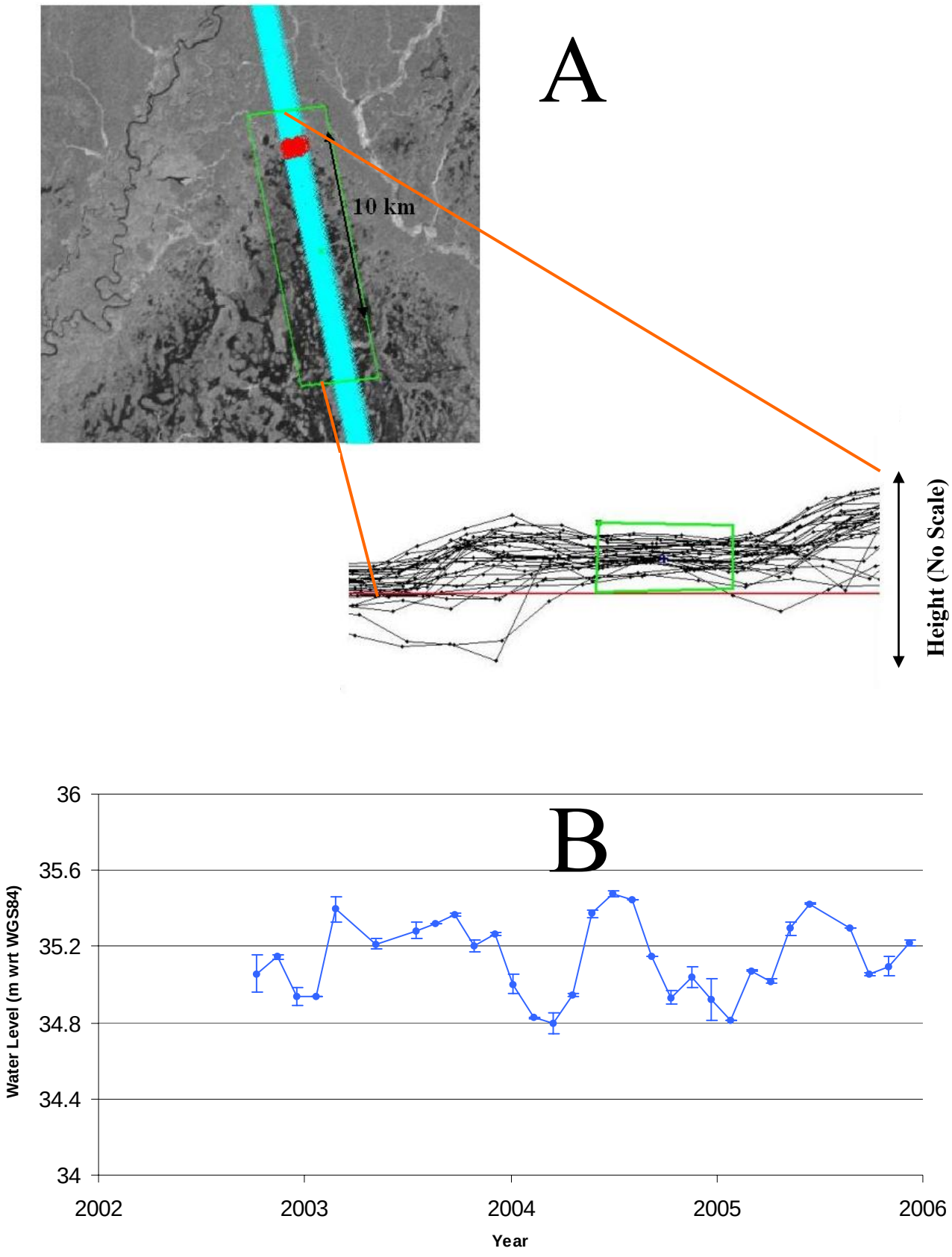
A
10 km
Height (No Scale)
B
Water Level (m wrt WGS84)
36
35.6
35.2
34.8
34.4
34
2002
2003
2004
2005
2006
Year

Figure 4

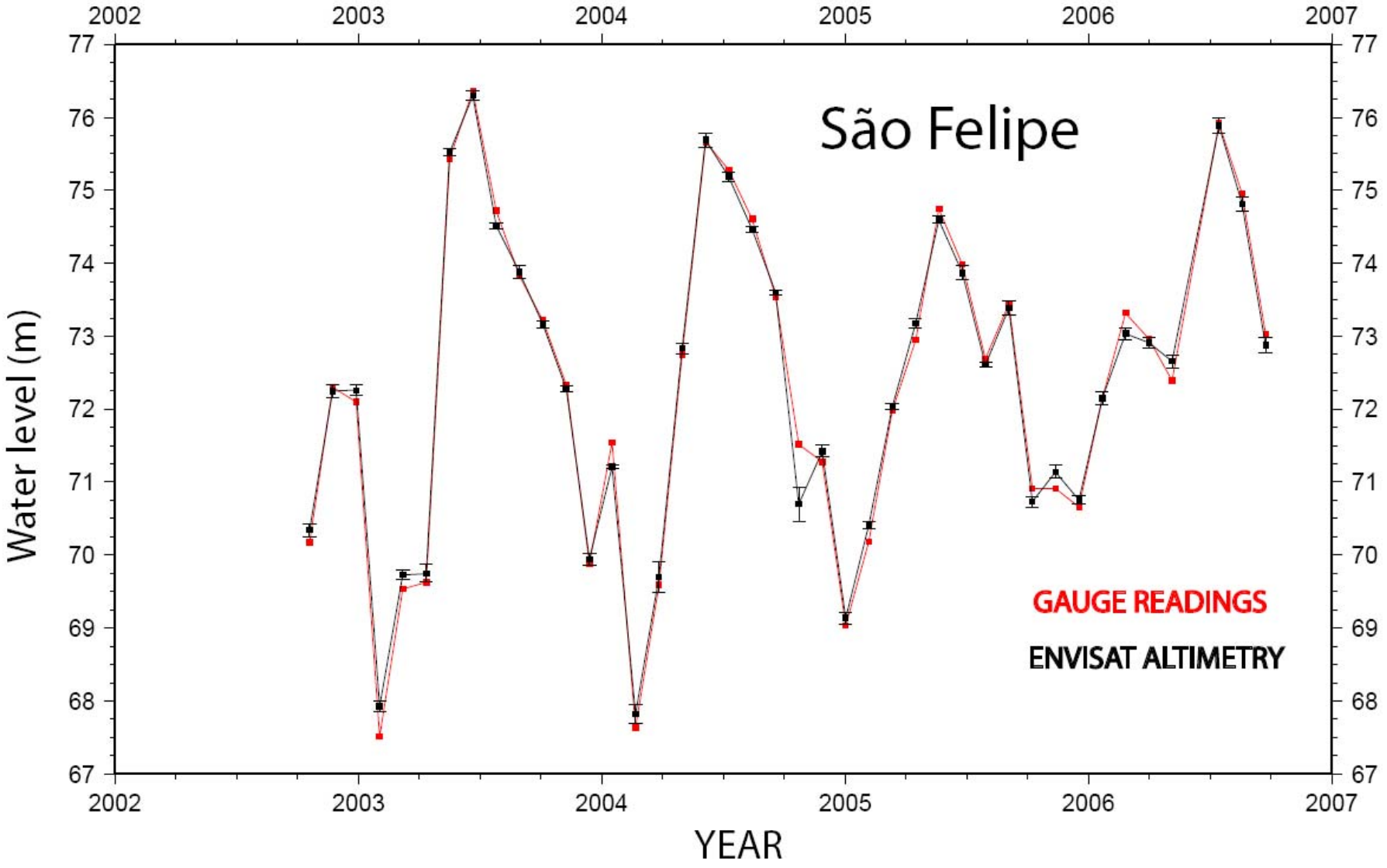
São Felipe
GAUGE READINGS
ENVISAT ALTIMETRY
Water level (m)
YEAR
2002
2003
2004
2005
2006
2007
67
68
69
70
71
72
73
74
75
76
77

Figure 5

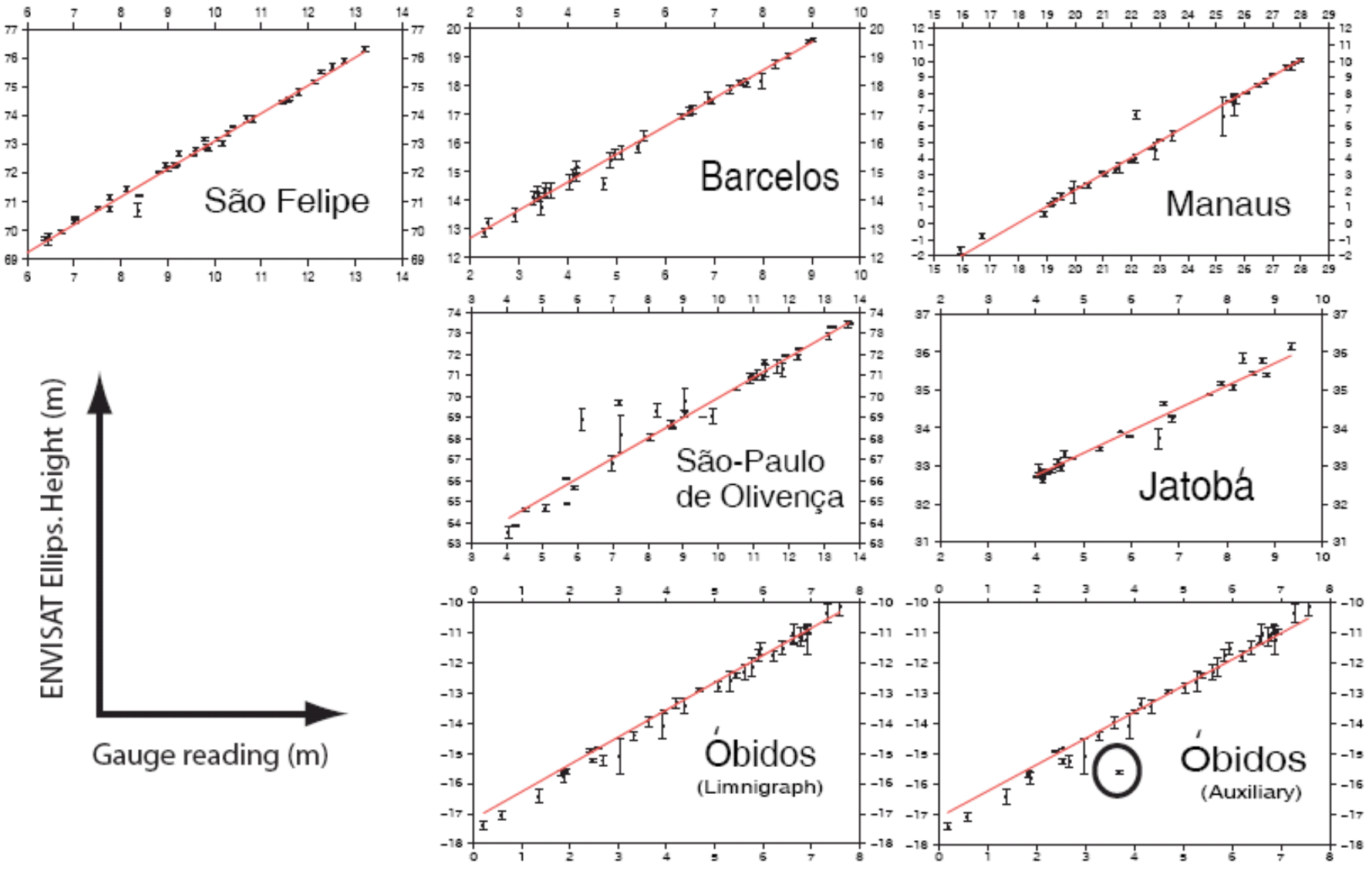
São Felipe
Barcelos
Manaus
São-Paulo
de Olivença
Jatobá
Óbidos
(Limnigraph)
Óbidos
(Auxiliary)
ENVISAT Ellips. Height (m)
Gauge reading (m)

Figure 6